J Mater Sci (2009) 44:2239–2246
DOI 10.1007/s10853-008-3199-4

FESTSCHRIFT IN HONOUR OF PROF T R ANANTHARAMAN ON THE OCCASION OF HIS 80TH BIRTHDAY

Methods to overcome embrittlement problem in 9Cr–1Mo ferritic steel and its weldment

Baldev Raj · S. Saroja · K. Laha · T. Karthikeyan · M. Vijayalakshmi · K. Bhanu Sankara Rao

Received: 7 May 2008 / Accepted: 15 December 2008 / Published online: 3 February 2009

Abstract This article presents the issues that need to be addressed in ferritic steel, for their use in nuclear core, namely, the embrittlement and type IV cracking of weldment. It has been established that the ferritic steels possess a significantly higher resistance to radiation damage as compared to the present generation austenitic stainless steels and the creep behavior is satisfactory for applications up to 873 K. The major challenges that need to be addressed are the poor creep resistance of the weld joints and embrittlement of ferritic steels. This article describes the efforts taken at IGCAR to overcome the embrittlement problem by impurity control, grain boundary engineering or design of suitable thermomechanical treatments in a 9Cr–1Mo ferritic steel.

Introduction

Rapid strides have been made world over in the design and development of advanced ferritic/martensitic steels by modification of chemistry and processing methods. The high chromium 9–12% ferritic/martensitic steels are being developed with continuous improvements in performance by optimization of carbon content, addition of solid solution strengtheners Mo and W, carbide forming elements Nb and V, partial substitution of Mo by W, and controlled addition of elements like N (0.03–0.05 wt%) and B for enhanced creep strength and stability of microstructure. Commercial steels like T91, T92, HT9, E911, and HCM12A show very high creep rupture strength and are proven materials for high-temperature applications. The new Cr–Mo–W steels are 'code approved' for thick section applications for operations up to 893 K [1]. Currently, modified 9Cr–1Mo steels, in which V and Nb contents have been optimized, are being used extensively for super heater tubings, headers, and pipings of conventional as well as nuclear power plants with steam temperatures up to 866 K [2, 3].

Ferritic steels are versatile due to their ability to possess a variety of microstructures, which can be produced by alloying additions and thermomechanical treatments imparting a range of properties. The steel in the normalized and tempered (N&T) condition has a tempered martensitic structure with a preponderance of monocarbides that impart the necessary creep strength, while the prior austenite grain and lath boundaries are decorated with Cr-rich $M_{23}C_6$ precipitates which increase the thermal stability of the steel [2, 3]. It is reported that thermal aging at temperatures above 773 K causes gradual but continuous degradation in upper shelf properties in addition to increase in the ductile-to-brittle transition temperature (DBTT) [4]. It is also well established that the fracture toughness of many power-plant steels deteriorate during service at elevated temperatures. These changes are due to two main reasons, namely, segregation of tramp elements to prior austenite grain boundaries which make the grain boundaries de-cohesive; and evolution of carbides and intermetallic phases, which cause progressive changes in the tempered martensitic microstructure and are prominent factors that deteriorate the fracture properties of the steel.

The 9–12%Cr steels perform well under irradiation in terms of void swelling, thermal and irradiation creep, and

B. Raj (✉) · S. Saroja · K. Laha · T. Karthikeyan · M. Vijayalakshmi · K. Bhanu Sankara Rao
Indira Gandhi Centre for Atomic Research, Kalpakkam 603 102, India
e-mail: dirsec@igcar.gov.in

S. Saroja
e-mail: saroja@igcar.gov.in

fatigue properties compared to their austenitic counter parts, which are crucial in achieving high burn-up in fast reactors. Currently, the 9–12%Cr steels are promising for high-temperature applications such as clad and wrapper of fast reactors. Although the 9–12% Cr–Mo steels have several attributes favoring them for core components, there are several challenges that need to be addressed. The major challenges are the reduced creep strength at temperatures higher than 823 K and reduction in toughness on irradiation to high displacement doses. For body centered cubic materials such as ferritic/martensitic steels, radiation hardening at low temperatures (<0.3 T_M) can lead to a large increase in the DBTT and lowering of impact energy even for low radiation dose such as 1 dpa (displacement per atom). The minimum operating temperature to avoid embrittlement in ferritic/martensitic (F/M) steels is ~473–523 K, while the upper limit is controlled by four different mechanisms: thermal creep, high-temperature helium embrittlement, void swelling, and compatibility with fuel and coolant. Void swelling is not expected to be significant in F/M steels up to damage levels of about 200 dpa [1]. In contrast, austenitic stainless steels show void swelling for a threshold level of 80 dpa itself. Hence, an imminent advantage in use of ferritic steels for core components is the increased residence time in the fast reactor, by few years (~6 years), as compared to austenitic steels (~1 year). The 12Cr steels, HT9, show a large shift (125 K) in DBTT as compared to modified 9Cr–1Mo steel (~54 K) [1]. An approach to reduce shift in DBTT is a major issue in ferritic steels for core component applications, and efforts to overcome this problem by selection of high purity metals, adoption of double or triple vacuum melting for steel making, strict control of tramp and volatile elements, and development of special processing methods, which would improve the nature of grain boundaries (grain boundary engineering), are in progress. The nature of embrittlement varies for different components of the reactor. For removable components such as clad, which are subjected to high temperature and pressure, with a residence time of a few years, creep embrittlement is the issue which decides their design and performance, while for permanent support structures increase in hardening and loss in fracture toughness on irradiation are major issues. The present article describes the efforts at Indira Gandhi Centre for Atomic Research in these directions.

Long-term microstructural stability of ferritic steels

The chemical composition of the modified 9Cr–1Mo steel being indigenously developed and supplied by MIDHANI Ltd., Hyderabad, India is given in Table 1. The chemistry is strictly controlled, more so for residuals like sulphur, phosphorus, and silicon. The inclusion content is kept low to maintain a high degree of cleanliness. The steel in the normalized and tempered condition consists of a tempered lath martensite structure. The grain and lath boundaries are decorated with carbides which were identified as Cr-rich $M_{23}C_6$ type using electron diffraction and energy dispersive X-ray analysis (EDX) on carbon extraction replica. Fine intralath monocarbides were identified as MX type (M = V, Nb and X = C, N); the details of analysis are presented elsewhere [5, 6]. The presence of Nb and V confers improved strength and creep resistance to the steel as compared to plain 9Cr–1Mo steel. Long-term microstructural stability in the temperature range of 773–873 K has been studied in our laboratory [5]. It is observed that the microstructure is stable up to 5000 h at 773 K beyond which Laves phase of $(Fe,Si)_2Mo$ type begin to form. The consumption of Mo in the Laves phase, although decreases the solid solution strengthening, can contribute to precipitation strengthening [7]. The presence of fine precipitates or layers of Laves phase could also offset the softening effect due to aging and are responsible for the reported loss of toughness or reduction in upper shelf energy in the steel [8].

The 9Cr–1MoVNb steel derives its creep strength from the solid solution strengthening, dislocation substructure strengthening, and precipitation strengthening. Molybdenum mostly confers solid solution strengthening to the steel. The creep strength of the alloy is significantly higher than the 2.25Cr–1Mo and plain 9Cr–1Mo steel for longer test durations, until about 873 K and is almost comparable to type 304 austenitic stainless steel [9]. However, the weld joints have always been the area of concern due to the heterogeneous microstructure [10], which is described below.

Table 1 Composition specification of the modified 9Cr–1Mo steel indigenously developed for PFBR

Element	C	Cr	Mo	Si	Mn	V	Nb	N	S
wt%	0.08–0.12	8.00–9.00	0.85–1.05	0.20–0.50	0.30–0.50	0.18–0.25	0.06–0.10	0.03–0.07	0.01 max.
	P	Cu	Ni	Al	Sn	Sb	Ti	Fe	
wt%	0.02 max.	0.10 max.	0.20 max.	0.04 max.	0.02 max.	0.01 max.	0.01 max.	Bal.	

Microstructural degradation of the weld joint due to precipitation of embrittling phases

The modified 9Cr–1Mo steel fusion weld joint due to thermal cycle produces a complex heterogeneous microstructure, consisting of base metal, deposited weld metal, and the heat-affected zone (HAZ) [11]. The base metal and weld metal consist of a tempered martensite structure, with columnar grains in the weld metal. The HAZ is comprised of coarse prior-austenitic grain martensite, fine prior-austenitic grain martensite, and an intercritical structure, as one traverse from the weld fusion interface toward the unaffected base metal. This is dictated by the peak temperatures experienced by the base metal during weld thermal cycle and the phase transformation characteristics of the steel. The room temperature microstructures in the intercritical region consist of a mixture of two phases, namely, martensite—the transformation product of the freshly formed austenite and the pre-existing tempered martensite. A complex residual stress also develops across the joint [12]. The weld joints of ferritic steels are generally subjected to a post-weld heat treatment (PWHT) at temperatures below Ac_1 not only to temper the martensite in the weld metal and HAZ, but also to relieve the residual stresses developed across the joint. A soft zone develops in the intercritical region on PWHT (Fig. 1), which has been rationalized as follows: Intercritical heating of the steel followed by quenching results in higher hardness than on subcritical heating (below Ac_1), since the austenite that forms on intercritical heating, transforms into martensite with high hardness on quenching, while the pre-existing tempered martensite is further tempered. The low temperatures in the intercritical range favor either coarsening of carbides or replacement by higher order ones, with no appreciable dissolution, thus resulting in a low-carbon austenite as compared to normalization process. While the low-carbon austenite transforms to martensite on cooling, PWHT at temperatures below Ac_1 results in much less secondary precipitation in the low-carbon martensite and far less in the heavily tempered ferrite. This enhanced recovery in the intercritical structure as compared to other regions of HAZ resulted in the soft zone in the weld joint (Fig. 1). During long-term thermal and creep exposures, a modified Z-phase, a complex Cr(V,Nb)N intergranular precipitate has been observed in the 9Cr–1MoVNb steel. Thus, intercritical heating during weld thermal cycle produces (i) recovery of martensitic lath structure resulting in subgrains with low dislocation density and coarsening of $M_{23}C_6$ precipitate (Fig. 2a) and (ii) enhanced precipitation of Z-phase (Fig. 2b) in the intercritical HAZ subsequently during creep exposure. It has been established that the localized microstructural degradation in the intercritical region of HAZ is mainly responsible for the premature creep rupture strength of Cr–Mo weld joint and can be overcome if weld residual stresses are adequately relieved by PWHT [13].

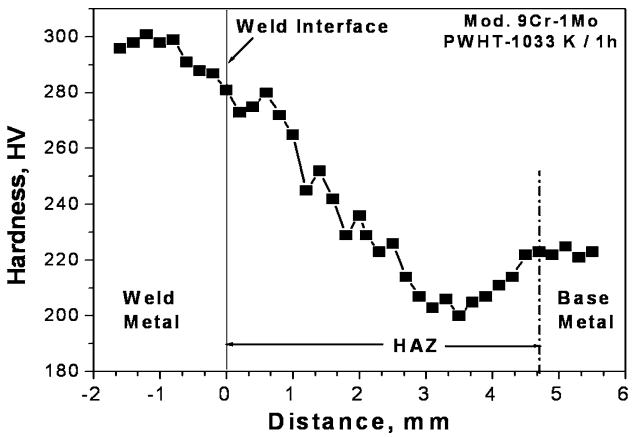

Fig. 1 Hardness variation across the weld joint of modified 9Cr–1Mo steel showing the formation of soft zone in the HAZ

The lower creep rupture strength of weld joint than the base metal is due to the different types of cracking developed during creep exposure [13, 14] (Fig. 3a). Four types of cracking have been identified in Cr–Mo steel weld joint. They have been categorized as Type I, Type II, Type III, and Type IV. The Type I and Type II crack originate in weld metal, propagate either through the weld metal itself (Type I) or cross over in the HAZ (Type II). The Type III cracking occurs in the coarse grain region of HAZ and can be avoided by refining the grain size. Type IV cracking nucleates and propagates in the intercritical/fine grain region of HAZ. At longer creep exposure and higher test temperature, the formation of microcracks by coalescence of nucleated cavities and propagation to the surface of the specimen produce type IV failure (Fig. 3b).

The type IV cracking susceptibility, defined as the reduction in creep rupture strength of weld joint compared to its base metal, depends on the type of ferritic steel. 2.25Cr–1Mo steel is most susceptible to type IV cracking; whereas the plain 9Cr–1Mo steel is the least susceptible. The relative unstable nature of Mo_2C which imparts creep strength to 2.25Cr–1Mo steel against thermal exposure drastically reduces the creep strength of the weld joint. The relatively higher type IV cracking susceptibility of modified 9Cr–1Mo steel as compared to 9Cr–1Mo at higher test temperature is related to the precipitation of Z-phase, in the former steel [11]. At elevated temperatures during long-term exposure, the Z-phase grows rapidly by dissolving the beneficial MX types of precipitates and accelerates the recovery in substructure with associated decrease in strength in the intercritical region of HAZ.

Although it is difficult to avoid Type IV cracking, several methods are being adopted to improve type IV cracking resistance [15–17]. It is more severe in thick

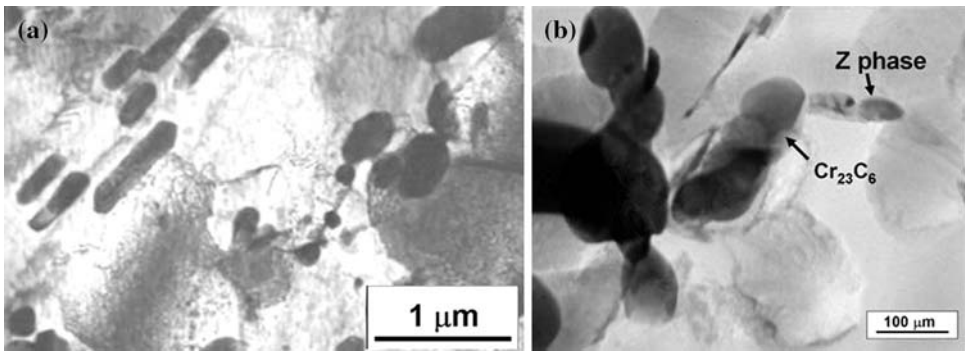

Fig. 2 TEM micrographs of intercritical HAZ of 9Cr–1MoVNb steel joint (creep tested at 923 K, 40 MPa, $t_r = 15{,}721$ h). **a** Subgrains and coarse $M_{23}C_6$ carbides. **b** Extraction replica showing presence of $M_{23}C_6$ and Z phase; EDX spectrum in inset shows enrichment of Cr, V, and Nb in Z-phase

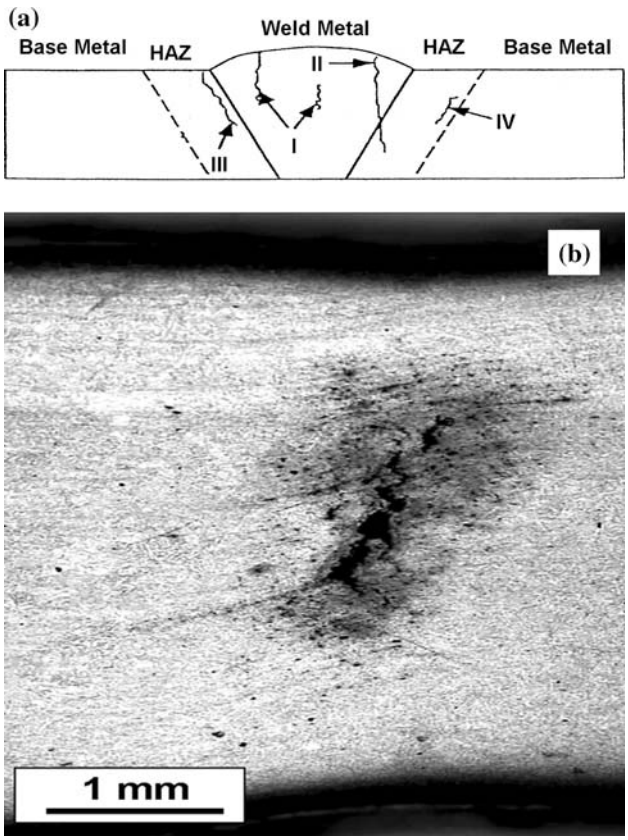

Fig. 3 **a** Types of cracking in weld joint of Cr–Mo steels on service exposure. **b** Type IV cracking in modified 9Cr–1Mo steel weld joint

sections due to the imposed geometrical constraint. A design modification can be adopted to decrease the variation in tensile stresses across the welded section of the component or avoid joints in critical regions having high system stresses and relocate them in the less critical region. Strength homogeneity across the weld joint can also be improved by normalizing the component after welding. An increase in width of the HAZ can reduce the stress triaxiality such that the soft intercritical region deforms with less constraint with the consequence of reduced creep cavitation, to minimize type IV cracking tendency. The width of the HAZ can be increased both by changing preheat and heat input during welding. Another contrasting approach to overcome type IV cracking is to avoid or minimize the width of the HAZ, to eliminate the intercritical zone. This is being attempted by employing advanced welding techniques such as laser welding. The resistance against intercritical softening can also be improved by increasing the base strength of the steel with the addition of solid solution hardening elements such as W, Re, and Co and also by microalloying the steel with boron. Microalloying with boron retards the coarsening rate of $M_{23}C_6$ by replacing some of its carbon. The boron content needs to be optimized with the nitrogen content to avoid BN formation. Addition of Cu is also found beneficial. Copper is almost completely insoluble in the iron matrix and when added in small amounts, precipitates as nano-size particles to impart creep resistance. A suitable adjustment of the chemical composition of steel within the specification range also reduces the large difference in creep strength between the softened HAZ, the base metal, and the coarse grain HAZ of the joint. A weld joint of modified 9Cr–1Mo steel with low carbon, nitrogen, and niobium has been reported [17] to possess creep strength comparable to that of the base steel.

Embrittlement issues in materials for clad and wrapper applications

In the long term, ferritic/martensitic steels (9–12% Cr) have been identified for clad and wrapper, due to their inherent low swelling behavior. The 9Cr–1Mo steel, modified 9Cr–1Mo (Grade 91), 9Cr–2Mo, and 12Cr–1MoVW (HT9) have low swelling rates even at doses up to 200 dpa [1] (HT9 shows a 1% swelling at 693 K for 200 dpa). However, the increase in the DBTT due to irradiation is a cause of serious concern for use of ferritic steels [18, 19]. Several methods have been attempted to address this problem, which includes modification of the steel through alloying additions, control of tramp elements by using pure raw materials and improved melting practices, and tailoring of microstructure through metallurgical treatments.

A viable approach for overcoming the reduction in fracture toughness is by grain refinement and grain boundary engineering [20]. Decrease in fracture toughness of HAZ in a ferritic joint, which is a serious concern, has been overcome by refinement of HAZ [21, 22] through suitable welding technique such as multi-pass fusion welding. In grain boundary engineering, thermomechanical treatments (TMT) are designed to increase the fraction of 'special' low energy boundaries in preference to the 'random' high energy boundaries, thereby reducing the impurity segregation and precipitation of embrittling phases at/near the boundaries [22]. The next section deals with the design of TMT.

Design of thermomechanical treatments and its effect on grain boundary characteristics

Figure 4 illustrates the philosophy behind the thermomechanical treatment adopted for 9Cr–1Mo ferritic steel. A deformation + recrystallization annealing is found to increase the fraction of 'coincidence site lattice (CSL)' boundaries in fcc materials [23]. A similar treatment consisting of mechanical deformation by different methods (forging/rolling) and recrystallization annealing (973 K/2 h) was adopted for 9Cr–1Mo steel. High strain/strain rates and cryo rolling treatments were also attempted to aid the formation of twins. Impurities tend to populate the highest energy boundaries such as prior-austenite grain boundaries. Hence, hot forging was one method designed to modify the prior-austenite grain boundaries. Since the steel is generally used in normalized and tempered condition, the deformation was followed by normalizing (1223 K/2 h/AC) and tempering (1023 K/2 h) (N&T). A lower

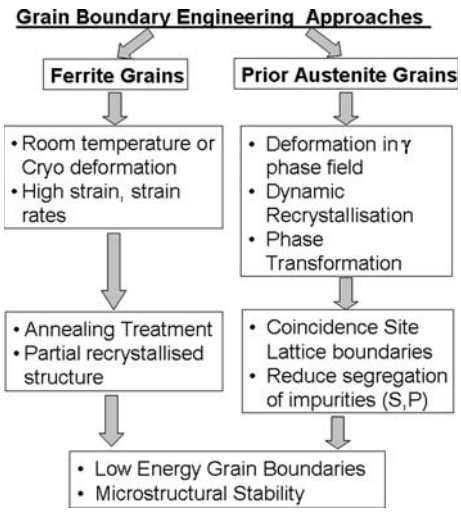

Fig. 4 Rationale for selection of thermomechanical treatments for grain boundary engineering in ferritic steels

austenitization temperature (35 K above Ac_3) was chosen to preserve the prior-deformation history.

Figure 5 shows the hardness data of the modified 9Cr–1Mo steel after different TMTs. The wide variation in hardness from 168 to 590 VHN suggests a significant modification of microstructure due to TMT. The conventional N&T treatment for the modified 9Cr–1Mo steel imparts a hardness of about 250 VHN. Hence, treatments that resulted in a similar hardness value, namely, 'cold forged,' 'cold forged and normalized,' and 'hot forged and N&T' were further studied by SEM-electron back scattered diffraction (EBSD) to evaluate the grain boundary character.

Figure 6 gives the results of the EBSD microtexture and grain boundaries for the N&T sample (reference). The grain boundaries were identified by the change in crystallographic orientation across adjacent grains. By comparing the experimental 'misorientation angle-rotation axis' of the grain boundary with the ideal CSL boundary and using the Brandon's criteria for allowable deviation, CSL boundaries from Σ3 to Σ29 were evaluated. The net amount of grain boundary energy in a material is dependent on both grain size and type of grain boundaries. The CSL boundaries have low specific surface energy compared to 'random boundaries,' while grain boundary surface would be more for a fine-grained material. A parameter called effective grain boundary energy (EGBE) [24], defined as

$$\mathrm{EGBE} = \frac{\left(\frac{4}{d}\right)\left[\left(\sum_{\text{for CSL 1}}^{29} Y_i F_i\right) + Y_{\max} F_{\mathrm{R}}\right]}{Y_{\max}},$$

$$Y_i = \left(1 - \frac{1}{\sum}\right) Y_{\max},$$

was evaluated for the samples. Here, F_i is the fraction of individual CSL boundaries, Y_i is the energy of CSL boundary, and $Y_{\max}$ is the energy of high angle random grain boundary. Table 2 gives the CSL fraction and the EGBE evaluated for the selected TMT samples. Compared to the reference N&T condition, the CSL fraction improved for the 'hot forged, N&T' condition alone, while it reduced for the cold-forged treatments. The EGBE is inversely related to grain size and hence is a strong function of grain size. The 'hot forged, N&T' steel exhibited a larger average grain size of 12 μm (higher than that of the reference condition) and resulted in the minimum value of EGBE. However, for a given grain size, special boundaries can reduce the propensity for precipitation, break the 'random boundary' network, and thereby resist grain boundary embrittlement. In austenitic stainless steels, resistance to sensitization and intergranular corrosion has been reported to be improved for both low (high fraction of special boundaries) and high (extreme randomisation of boundaries) values of EBGE, while it is poor for intermediate

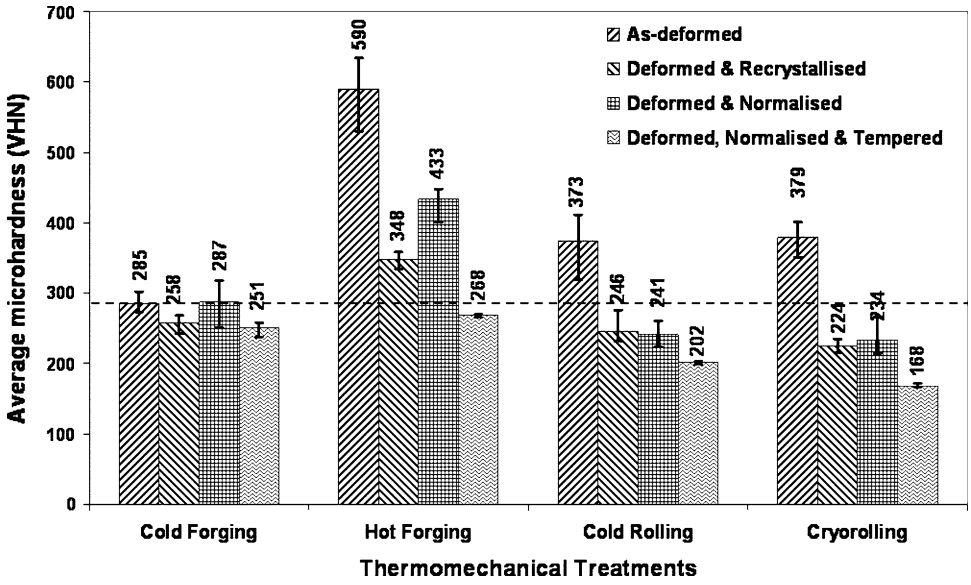

Fig. 5 Hardness variation in modified 9Cr–1Mo ferritic steel subjected to different thermomechanical treatments, compared with the hardness of the N&T steel (*dotted line*)

EGBE values [24]. Efforts are in progress to correlate the EGBE to DBTT and identify the optimum EGBE that could lead to reduction in DBTT. The effect of grain size on DBTT is already well established and has also been demonstrated in our laboratory for the 9Cr–1Mo steel [21, 22].

Evaluation of threshold fraction of CSL boundaries to avoid intergranular crack propagation using percolation model

The task of experimentally characterizing and relating the crack propagation with grain boundary distribution is tedious. Modeling of crack propagation in a simulated three-dimensional Poisson–Voronoi grain structure was carried out to evaluate the critical amount of strong boundaries required to stop the crack connectivity along weak boundaries [25]. The percolation threshold, to break the connectivity along 'random boundaries,' in a one-dimensional crack network is $\sim$0.8 [25]. This provides a conservative target of fraction of 'CSL boundaries' required to prohibit intergranular crack phenomena. Since the crack is a two-dimensional (2D) feature, threshold fraction of 'special boundaries' required to break a 2D network of 'random boundaries' is more relevant. This criterion would give the lower bound estimate of 'CSL boundaries' fraction required for preventing the intergranular crack. The percolation thresholds for 2D and 1D grain boundary connectivity are complementary [26]. Thus, the percolation threshold to break a 2D network of 'random boundaries' is $\sim$0.2. In the above geometrical models, the thorough interconnectivity of 'random boundaries' is taken as the criteria for intergranular crack susceptibility and the grain size has no effect. However, it is known that a finer grain size imparts improved resistance to inter- and transgranular mode of crack propagation as the crack path would be tortuous. The fracture process is composed of crack initiation and crack propagation stages. The crack initiation primarily dictates the failure and there exists a threshold size of flaw/crack for a given applied stress. When the crack size is greater than a critical value, crack would propagate to failure. The interconnected 'random boundaries' can be considered as inherent flaws present in the material acting as crack initiation sites. The susceptibility to intergranular crack can be assessed based on the maximum size of interconnected 'random boundaries' cluster and the geometrical model can be improved to incorporate the effect of both grain size and fraction of 'special boundaries.' Work is in progress in this direction to estimate the susceptibility of the 9Cr–1Mo ferritic steel to intergranular fracture based on experimentally determined grain boundary characteristics.

Conclusion

The article has identified two important embrittlement issues in 9Cr–1Mo ferritic steel, namely, the creep embrittlement in weld joint and reduction in fracture toughness due to microstructural changes on service exposure. Type IV cracking in weld joint, which is an important issue governing creep strength, and ductility of Cr–Mo ferritic steel is associated with pronounced localization of creep deformation and cavitation in the soft intercritical region of HAZ, leading to premature failure. The micromechanism leading to soft zone formation in the intercritical region of HAZ in modified 9Cr–1Mo steel has been identified, which is associated with the recovery of the tempered martensite microstructure. Creep strength

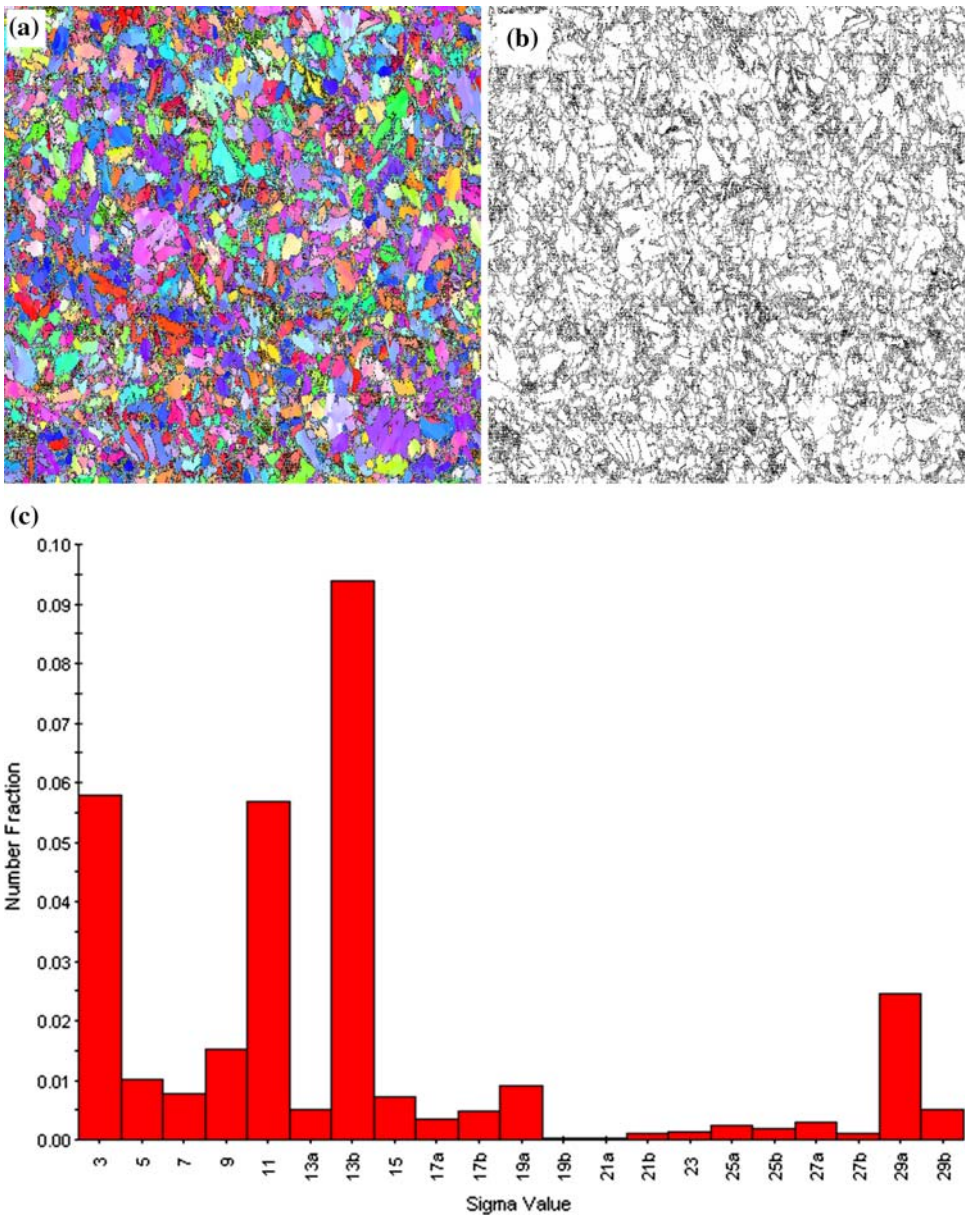

Fig. 6 **a** EBSD crystal orientation map of the normalized and tempered-modified 9Cr–1Mo ferritic steel. **b** Grain boundary map showing the random boundaries (*grey*) and CSL, low angle boundaries (*black*). **c** Fraction of CSL boundaries chart for $\Sigma 3-29$ type

Table 2 Grain size, CSL fraction, and the EGBE for the different TMT samples and the reference sample

Sample	Average grain size (μm)	CSL fraction	EGBE (μm^{-1})
N&T	6.23	0.3276	0.5675
Cold forged	7.29	0.1660	0.5266
Cold forged & N	5.49	0.2048	0.6909
Hot forged, N&T	12.05	0.3408	0.2925

heterogeneity across the weld joint induces type IV cracking and reduction of strength heterogeneity by adopting appropriate welding procedures and by microalloying in the steel are methods to reduce the susceptibility to type IV cracking. The second serious issue in ferritic steel for their employment as core component material is the reduction in fracture toughness due to exposure to high temperature and irradiation. Using a geometrical grain model, the fraction of crack-resistant boundaries required to break the 1D and 2D crack percolation was found to be 20% and 80%, respectively. An attempt using grain boundary engineering by optimum thermomechanical treatments has been made to overcome the susceptibility of ferritic steels to temper/irradiation embrittlement. The 'hot forged, N&T' treatment was found to improve the CSL fraction and also reduce the EGBE, as compared to the conventional N&T treatment in a modified 9Cr–1Mo steel.

Acknowledgements The authors thank all their colleagues who have been part of the material development activities at Indira Gandhi Centre for Atomic Research, Kalpakkam.

References

1. Klueh RL (2005) Int Mater Rev 50(5):287
2. Vitek JM, Klueh RL (1983) Metall Mater Trans A 14:1047
3. Jones BW, Hills CR, Polonis DH (1991) Metall Trans A 22:1049
4. Klueh RL, Vitek JM (1989) J Nucl Mater 161:13
5. Thomas Paul V, Saroja S, Vijayalakshmi M (2008) J Nucl Mater 378:273
6. Thomas Paul V, Saroja S, Hariharan K et al (2007) J Mater Sci 42:5700. doi:10.1007/s10853-006-0704-5
7. Hippsley CA, Haworth NP (1988) Mater Sci Technol 4:791
8. Wall M, Lane CE, Hippsley CA (1994) Acta Metall 42:1295
9. Fujita T (1992) ISIJ Int 32(2):175
10. Chandravathi KS, Laha K, Bhanu Sankara Rao K et al (2001) Mater Sci Technol 17:559
11. Laha K, Chandravathi KS, Parameswaran P et al (in press) Metall Mater Trans A. doi:10.1007/s11661-008-9724-x
12. Browne RJ, Cane BJ, Parker JD et al (1981) In: Wilshire B et al (eds) Creep and fracture of engineering materials and structures. Pineridge Press, Swansea, p 645
13. Laha K, Chandravathi KS, Parameswaran P et al (2007) Metall Mater Trans A 38:58
14. Shüller HJ, Haigh L, Woitscheck A et al (1974) Der Machinenschaden 47:1
15. Morinaga M, Hashizume R, Murata Y et al (1974) In: Coutsouradis D et al (eds) Materials for advanced power engineering, part 1. Kluwer Academic Publishers, Dordrecht
16. Abe F, Tabuchi M, Kondo M et al (2007) Int J Pressure Vessels Piping 84:44
17. Abe N, Kunisada Y, Sugiyama T et al (1990) Rivita Italian delta Saldatura 2:44
18. Kohyama A, Hishinuma A, Gelles DS et al (1996) J Nucl Mater 233–237:138
19. Klueh RL, Alexander DJ (1992) J Nucl Mater 187:60
20. Watanabe T, Tsurekawa S (2004) Mater Sci Eng A 387–389:447
21. Moitra A, Sreenivasan PR, Parameswaran P et al (2002) Mater Sci Technol 18:1195
22. Moitra A, Parameswaran P, Sreenivasan PR et al (2002) Mater Charact 48:55
23. Randle V (2004) Acta Mater 52:4067
24. Wasnik DN, Kain V, Samajdar I et al (2002) Acta Mater 50:4587
25. Karthikeyan T, Saroja S, Vijayalakshmi M et al (2007) In: Raj B, Ranganathan S, Mannan SL et al (eds) Frontiers in design of materials. University Press (India) Private Limited, Hyderabad, p 109
26. Frary M, Schuh CA (2005) Philos Mag A 85(11):1123